Monetite Formed in Mixed Solvents of Water and Ethylene Glycol and Its Transformation to Hydroxyapatite

Ming-Guo Ma, Ying-Jie Zhu,* and Jiang Chang

State Key Laboratory of High Performance Ceramics and Superfine Microstructure, Biomaterials and Tissue Engineering Research Center, Shanghai Institute of Ceramics, Chinese Academy of Sciences, Shanghai 200050, People's Republic of China, and Graduate School of Chinese Academy of Sciences, People's Republic of China

Received: March 20, 2006; In Final Form: May 29, 2006

Agglomerated nanorods of hydroxyapatite have been synthesized using monetite as a precursor in a NaOH solution. Monetite consisting of nanosheets has been successfully synthesized by a one-step microwave-assisted method using $CaCl_2 \cdot 2.5H_2O$, NaH_2PO_4, and sodium dodecyl sulfate (SDS) in water/ethylene glycol (EG) mixed solvents. The effects of the molar ratio of water to EG and the reaction time on the products were investigated. The products were characterized by X-ray powder diffraction (XRD), scanning electron microscopy (SEM), transmission electron microscopy (TEM), and Fourier transform infrared spectrometry (FTIR).

Introduction

Calcium phosphates including hydroxyapatite (HA) are bioactive materials, which have the potential to be used as bone substitutes.[1] However, the bioactivity, biocompatibility, stability, and mechanical properties of calcium phosphates are determined by their morphology, crystallite size, composition, and structure. Therefore, the control over the morphology of calcium phosphates, especially HA, is of great importance for their bioapplications.

Much effort has been placed on the synthesis of calcium phosphates and HA.[2−11] For example, Imai et al.[6] prepared nanotextured and nanofibrous HA using dicalcium phosphate and gelatin. Zhan et al.[7] synthesized HA nanorods using $Ca(NO_3)_2 \cdot 4H_2O$, $NaH_2PO_4 \cdot 2H_2O$, urea, and gelatin in an aqueous solution at 100 °C for 4 days. Tas et al.[8] reported the synthesis of Na- and K-doped brushite and its conversion to carbonated apatite at 37 °C by simply soaking the powders in simulated body fluid solutions. The appropriate template or additive was also used to control the morphology of calcium phosphates, especially HA. Liu et al.[9] studied the effect of chondroitin sulfate on the crystallization of HA nanocrystallites. Tam et al.[10] used a double-hydrophilic block copolymer as the template for the controlled precipitation of calcium phosphate from aqueous solution at various pH values. Zhu et al.[11] studied the influence of the reaction conditions and glutamic acid on the morphology of HA with partial substitution of fluorine by hydrothermal methods for 24 h.

Monetite ($CaHPO_4$) is also bioactive.[12,13] Monetite was usually used as a precursor to synthesize HA.[4,5] It is difficult to control the morphology of HA because a nanoneedlelike morphology is usually formed. The control over the morphology of monetite to obtain the specific morphology of HA is a useful route. The development of simple, fast, and low-cost synthesis methods for control over the morphology of monetite and HA is of great importance for broadening and improving its biomedical applications. At a pH above 9, the most stable phase is HA; however, monetite is stable under acidic conditions (pH below 4.8).[14] There has been only a few reports on the synthesis of monetite. For example, Yoshimura et al.[15] reported hydrothermal synthesis of monetite whiskers and HA needles from monocalcium phosphate monohydrate at 160 and 200 °C for 4 h. Yoshimura et al.[16] synthesized crystalline whiskers of HA by the hydrothermal treatment of β-tricalcium phosphate (β-TCP) and citric acid, but monetite crystals were obtained at a lower temperature and pressure. Hsu et al.[17] used sintered HA as a substrate for hydrothermal reaction, and monetite could be deposited on the surface of HA at 200−300 °C. Cui et al.[18] reported the preparation of nanosized needlelike monetite in reverse microemulsions. Gibson et al.[19] synthesized a coating of crystalline monetite on titanium substrates by electrochemical methods and studied the transformation of monetite to HA by immersion in alkaline solutions. The effect of carbonate on the crystallinity and morphology of the apatite crystallites during the conversion of monetite to apatite was also reported.[20]

Microwave heating is a promising technology whose applications in materials fields have been rapidly growing[21−25] due to its unique effects as compared with conventional heating, such as rapid volumetric heating, increased reaction rates and shortened reaction times, enhanced reaction selectivity, and energy saving. Despite these advantages, there have been only a few reports on the microwave-assisted synthesis of monetitie and HA. Vaidhyanathan and Rao[26] reported the synthesis of HA using a microwave-assisted method. Torrent-Burgues et al.[27] synthesized HA with a needlelike morphology using Ca/citrate/phosphate solutions by microwave heating. Tas et al.[28] produced HA, tricalcium phosphate (TCP), and biphasic HA-TCP nanowhiskers by a microwave-assisted combustion synthesis/molten salt synthesis hybrid route.

To the best of our knowledge, there has been no report on the synthesis of flowerlike monetite by the microwave-assisted method. In this work, monetite with a flowerlike morphology consisting of nanosheets has been successfully synthesized by a one-step microwave-assisted method using $CaCl_2 \cdot 2.5H_2O$,

* Corresponding author. Phone: 86-21-52412616. Fax: 86-21-52413122. E-mail: y.j.zhu@mail.sic.ac.cn.

10.1021/jp061738r CCC: $33.50
Published on Web 07/06/2006

NaH_2PO_4, and sodium dodecyl sulfate (SDS) in water/ethylene glycol (EG) mixed solvents. The transformation of monetite to HA has been realized in NaOH solution.

Experimental Procedures

All chemicals were of analytical grade reagents and used as received without further purification. All experiments were conducted under air atmosphere. In a typical experiment, 0.200 g of sodium dodecyl sulfate (SDS) was dissolved in mixed solvents of 20 mL of ethylene glycol (EG) and 3 mL of deionized water in a 50-mL round-bottomed flask under magnetic stirring. Then, 0.229 g of calcium chloride ($CaCl_2 \cdot 2.5H_2O$) and 0.193 g of NaH_2PO_4 were dissolved into the solution. The Ca/P molar ratio in the starting solution was equal to 0.91. The solution was heated to 95 ± 2 °C and kept at this temperature for 1 h by microwave heating. The microwave oven used was a focused single-mode microwave synthesis system (Discover, CEM) equipped with a magnetic stirrer and a water-cooled condenser. The temperature was controlled by automatic adjusting of microwave power. The product was separated from the solution by centrifugation at a speed of 10 000 rpm, washed by ethanol several times, and dried at 60 °C in a vacuum of 60 Pa. Finally, white powder was obtained. The samples were kept in plastic vials and placed in a vacuum desiccator.

X-ray powder diffraction (XRD) patterns were recorded on a Rigaku D/MAX 2550 X-ray diffractometer with a graphite monochromator and Cu Kα radiation ($\lambda = 1.54178$ Å) operating at 40 kV and 100 mA with a step size of 0.02° at a scanning rate of 0.12° s^{-1} in 2θ range from 10 to 70°. Scanning electron microscopy (SEM) micrographs were recorded on a JXA-8100 scanning electron microscope. All samples were Au coated with a thickness of ∼20 nm prior to examination by SEM. Transmission electron microscopy (TEM) micrographs were recorded on a JEOL JEM-2100F field emission transmission electron microscope with an accelerating voltage of 200 kV. Samples were deposited on thin amorphous carbon films supported by copper grids from ultrasonically processed ethanol solutions. Fourier transform infrared (FTIR) spectroscopy was carried out with a Thermo Nicolet Nexus spectrometer, using the KBr disk method.

Results and Discussion

Figure 1 shows the XRD pattern of a typical sample synthesized by microwave heating $CaCl_2 \cdot 2.5H_2O$, NaH_2PO_4, and SDS in mixed solvents of water (3 mL) and EG (20 mL) at 95 ± 2 °C for 1 h. It indicates that the sample consisted of a single phase of crystalline monetite with a triclinic structure (ICDD 75-1520). The chemical reaction for the formation of monetite can be simplified as follows:

$$Ca^{2+} + H_2PO_4^- = CaHPO_4 + H^+$$

The morphologies of the samples were investigated by SEM. Figure 2 shows SEM micrographs of the sample synthesized under microwave heating at 95 ± 2 °C for 1 h using SDS, from which one can see monetite with flowerlike and bundlelike morphologies. Each flowerlike or bundlelike microstructure was formed by the assembly of nanosheets with thicknesses ranging from 80 to 100 nm and with lateral sizes up to 3.5 μm. Figure 2b is a typical flowerlike morphology of monetite.

Figure 3 shows TEM micrographs of some incomplete assemblies of monetite nanosheets. Figure 3f show a typical bundlelike monetite assembled from nanosheets. From Figure 3a−e, one can see the evolution process of the flowerlike monetite. Considering the previous experiment result, we propose that the growth mechanism of monetite may follow the oriented attachment mechanism.[29−32]

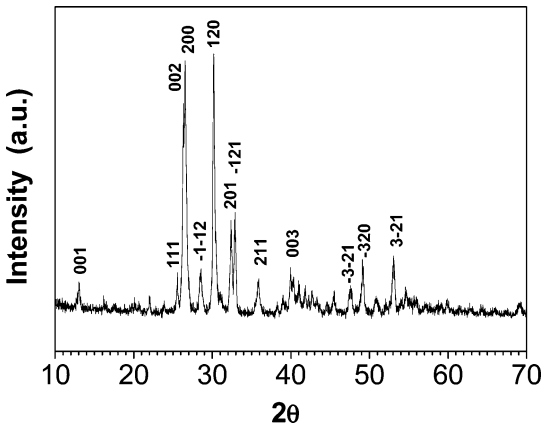

Figure 1. Typical XRD pattern of monetite powder prepared by microwave heating at 95 ± 2 °C for 1 h.

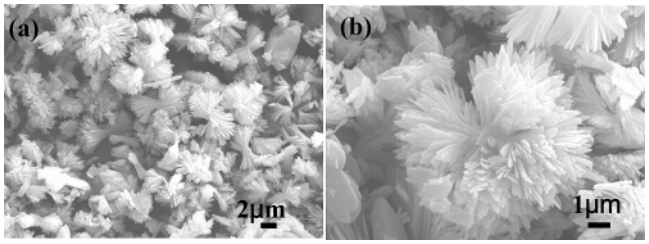

Figure 2. SEM micrographs of monetite prepared by microwave heating at 95 ± 2 °C for 1 h: (a) at a low magnification and (b) at a high magnification.

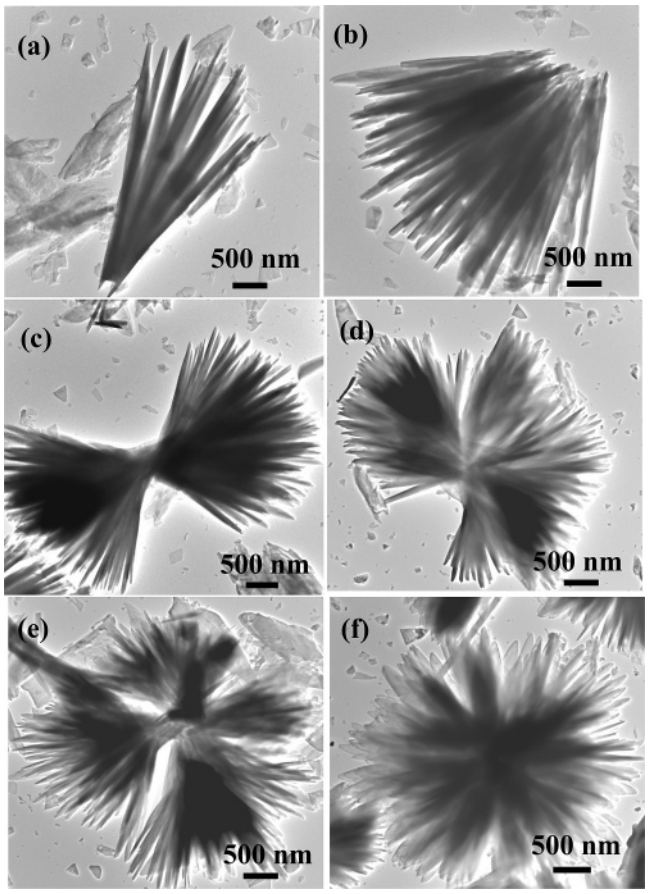

Figure 3. TEM micrographs of monetite prepared by microwave heating at 95 ± 2 °C for 1 h.

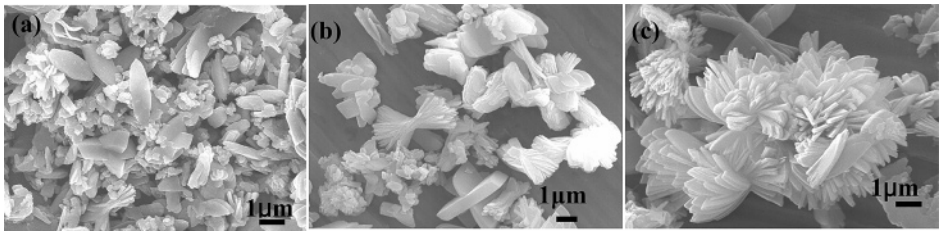

Figure 4. SEM micrographs of monetite prepared by microwave heating at 95 ± 2 °C for different times. (a) 1 min; (b) 5 min; and (c) 20 min.

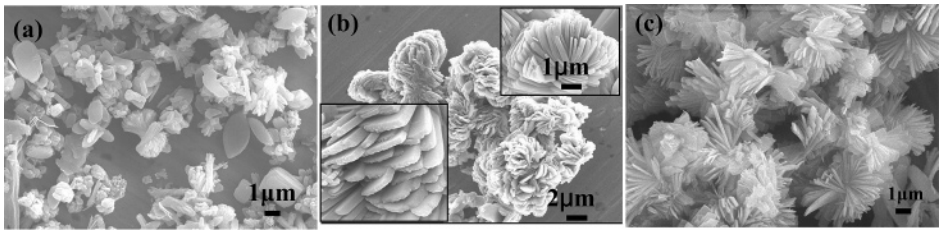

Figure 5. SEM micrographs of monetite prepared by microwave heating at 95 ± 2 °C for 1 h at different ratios of water to EG: (a) water (1 mL)/EG (20 mL); (b) water (5 mL)/EG (20 mL), the top inset of panel b shows a single flowerlike morphology, and the bottom inset of panel b shows the detailed structure of a flowerlike morphology; and (c) water (10 mL)/EG (20 mL).

To investigate the formation mechanism of flowerlike monetite, the monetite samples were prepared at 95 ± 2 °C for different heating times, while other reaction conditions were the same. When the heating time was 1 min (Figure 4a), many irregular polyhedra and spindlelike nanosheets were observed. Only a few low-symmetry bundlelike monetites were observed, and the degree of assembly was low. When the heating time was increased to 5 min, the congeries and bundles of nanosheets dominated (Figure 4b). When the heating time was increased to 20 min, the highly oriented nanosheets were assembled to form the flowerlike morphology (Figure 4c). The degree of assembly increased with increasing time, although the sizes of the monetite structures increased. From Figure 4a−c, one can clearly see the process of oriented-aggregation-based growth from nanosheets to a flowerlike morphology.

The ratio of water to EG had a significant effect on the size and morphology of monetite. When the ratio of water to EG was 3:20 (Figure 2), the flowerlike morphology was obtained. However, when the ratio of water to EG was 1:20, the majority was sheets, and a small number of bundles was also observed (Figure 5a). When only EG was used as the solvent, irregular morphologies were obtained, and no bundles were observed. By increasing the ratio of water to EG, a flowerlike morphology formed (Figure 5b,c). When only water was used as the solvent, flakes were obtained. Therefore, mixed solvents of EG and water are favorable for the formation of a flowerlike morphology of monetite.

SDS was used as a surfactant to control the morphology of the monetite. SDS is favorable for the formation of a flowerlike morphology of monetite. In the absence of SDS, the morphologies of monetite were sheets and a small number of bundles. No flowerlike morphology was obtained. However, the flowerlike and bundlelike morphologies were formed in the presence of SDS. Becasue of the electrostatic interaction with Ca^{2+} ions, the negatively charged SDS polar groups acted as active sites for the nucleation of monetite. Ca^{2+} ions strongly adsorbed on the micellar surface of the opposite charge, leading to a much faster nucleation rate on the surface of the SDS micelles. Because of the high viscosity of EG at room temperature, the diffusion of Ca^{2+} and HPO_4^{2-} ions and fast nucleation were restrained. With the elevation of temperature by microwave heating, the viscosity of EG rapidly decreased, and the polarization of EG and water molecules under the rapidly changing electric field of the microwave reactor may facilitate the anisotropic growth of monetite nanosheets. The flowerlike morphology was formed by the assembly of nanosheets with the help of SDS through the oriented attachment mechanism.

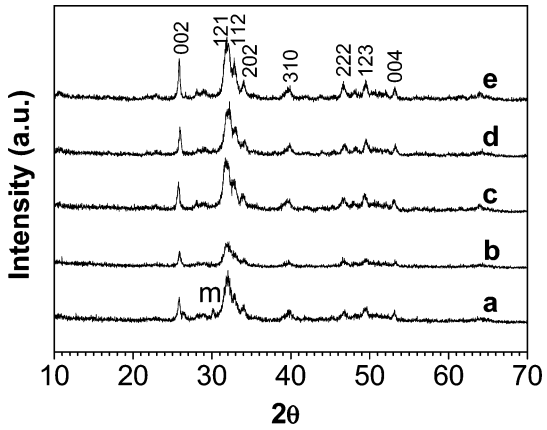

Figure 6. XRD patterns of the samples prepared by immersing flowerlike monetite powder in 0.1 M NaOH solution at 60 °C for different times: (a) 15 min; (b) 1 h; (c) 4 h; (d) 8 h; and (e) 12 h (m stands for monetite). The flowerlike monetite was prepared under the same conditions as in Figure 2.

Monetite is an excellent precursor for the formation of HA. We used flowerlike monetite as a precursor to obtain HA. Figure 6 shows the XRD patterns of samples prepared by immersing flowerlike monetite powder in 0.1 M NaOH solution at 60 °C for 15 min and 1, 4, 8, and 12 h, respectively. The XRD pattern of the monetite sample immersed in NaOH solution for 15 min indicates the presence of HA with the hexagonal structure (ICDD 84-1998) as a major phase and a minor phase of the residual monetite (Figure 6a). The XRD pattern presented in Figure 6b, corresponding to the monetite sample immersed in NaOH solution for 1 h, shows a single phase of crystalline HA. The transformation from monetite to HA was complete within 1 h, which was much shorter than previously reported (4 h).[19] The pH values of the solutions for the hydroxyapatite samples prepared for 15 min and 1, 4, and 8 h were 12.48, 12.45, 12.40, and 12.40, respectively.

The FTIR spectra (Figure 7) were used to identify the functional groups of the samples. Figure 7a shows the FTIR

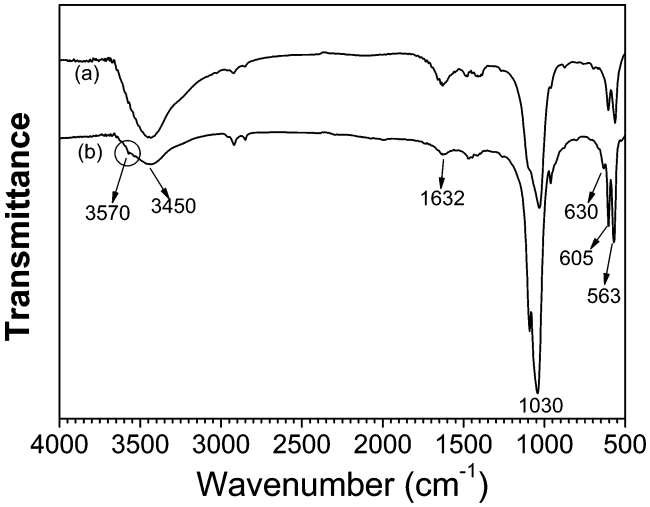

Figure 7. FTIR spectra of the samples prepared: (a) by immersing monetite powder in 0.1 M NaOH solution at 60 °C for 1 h; (b) by calcination of the product obtained in (a) at 800 °C for 3 h.

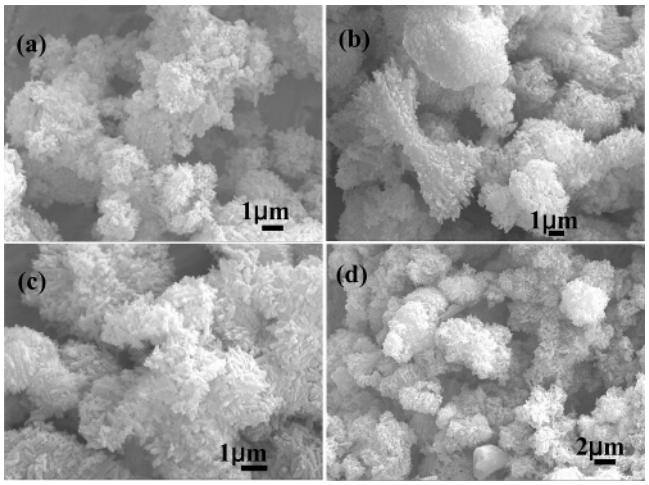

Figure 8. SEM micrographs of HA prepared by immersing monetite powder in 0.1 M NaOH solution at 60 °C for (a) 15 min; (b) 1 h; (c) 4 h; and (d) 8 h.

spectrum of the sample prepared by immersing the monetite powder in a 0.1 M NaOH solution at 60 °C for 1 h. The broad strong peak with a maximum at around 3450 cm^{-1} is assigned to the adsorbed water in hydroxyapatite.[33] The characteristic stretching mode of the OH- vibration in hydroxyapatite is located at around 3570 cm^{-1},[34] which is not clearly observed in Figure 7a because of the overlapping with the strong band at around 3450 cm^{-1} due to the adsorbed water.[33] However, a peak at about 3570 cm^{-1} appeared after the calcination of the product obtained by immersing monetite powder in the NaOH solution at 800 °C for 3 h (Figure 7b), indicating the presence of a hydroxyl group in the apatite. The band at ∼1632 cm^{-1} is assigned to the bending mode of the OH- vibration. The band at 630 cm^{-1} belongs to the liberation mode of the OH- vibration (Figure 7b).[34] The intense peaks located at 1030, 605, and 563 cm^{-1} are assigned to PO_4^{3-}.[35] On the basis of the XRD and FTIR results, we can conclude that the samples obtained by immersing monetite powder in the NaOH solution are hydroxyapatite.

Figure 8 shows SEM micrographs of HA samples after immersion of the monetite powder in a NaOH solution at 60 °C for 15 min and 1, 4, and 8 h, respectively. One can see the agglomerated nanorods of HA. The sizes of the HA nanorods

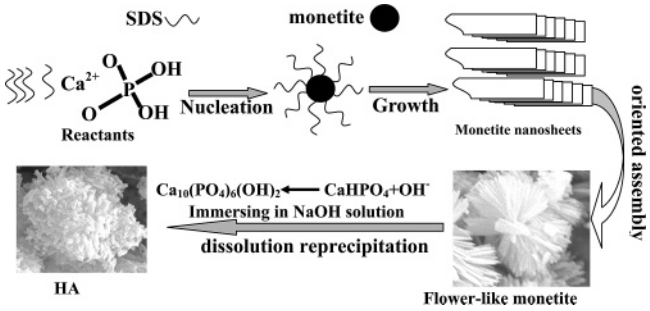

Figure 9. Schematic representation of the formation process of HA.

increased with increasing the immersing time in the NaOH solution. This interesting result indicates that it is feasible to prepare the agglomerated nanorods of HA through the conversion of the monetite in NaOH solution, providing a simple route to the synthesis of HA.

Figure 9 illustrates the formation process of the monetite with a flowerlike morphology and its transformation to HA. The mechanism for the transformation of monetite to HA in the NaOH solution can be explained by a continuous process of dissolution and a reprecipitation mechanism. The monetite was continuously dissolved and produced Ca^{2+} and PO_4^{3-} ions because the high pH destroyed the thermodynamic equilibrium of monetite. The HA reprecipitated and crystallized at the surface of the monetite to form HA. This mechanism was also proposed by Da Silva et al.[19] for the transformation of monetite to HA in bioactive coatings on titanium.

Conclusion

In summary, the microwave-assisted method has been successfully used for the synthesis of monetite with flowerlike and bundlelike morphologies using $CaCl_2 \cdot 2.5H_2O$ and NaH_2PO_4 in the presence of SDS in mixed solvents of water and EG. The molar ratio of water to EG and the reaction time have a significant effect on the size and morphology of monetite. The agglomerated nanorods of hydroxyapatite can be obtained through immersion of monetite powder in the NaOH solution. This method is simple and low-cost for the production of flowerlike monetite and agglomerated nanorods of hydroxyapatite.

Acknowledgment. Financial support from the National Natural Science Foundation of China (50472014), the Chinese Academy of Sciences under the Program for Recruiting Outstanding Overseas Chinese (the Hundred Talents Program), and the National Basic Science Research Program of China (973 Program) (Grant 2005CB522700) is gratefully acknowledged.

References and Notes

(1) Weiss, P.; Obadia, L.; Magne, D.; Bourges, X.; Rau, C.; Weitkamp, T.; Khairoun, I.; Bouler, J. M.; Chappard, D.; Gauthier, O.; Daculsi, G. *Biomaterials* **2003**, *24*, 4591−4601.

(2) Sundaram, N. M.; Girija, E. K.; Ashok, M.; Anee, T. K.; Vani, R.; Suganthi, R. V.; Yokogawa, Y.; Kalkura, S. N. *Mater. Lett.* **2006**, *60*, 761−765.

(3) Zhao, Y. F.; Ma, J. *Microporous Mesoporous Mater.* **2005**, *87*, 110−117.

(4) Shih, W. J.; Chen, Y. H.; Wang, S. H.; Li, W. L.; Hon, M. H.; Wang, M. C. *J. Cryst. Growth* **2005**, *285*, 633−641.

(5) Lin, K. S. K.; Tseng, Y. H.; Mou, Y.; Hsu, Y. C.; Yang, C. M.; Chan, J. C. C. *Chem. Mater.* **2005**, *17*, 4493−4501.

(6) Furuichi, K.; Oaki, Y.; Imai, H. *Chem. Mater.* **2006**, *18*, 229−234.

(7) Zhan, J. H.; Tseng, Y. H.; Chan, J. C. C.; Mou, C. Y. *Adv. Funct. Mater.* **2005**, *15*, 2005−2010.

(8) Tas, A. C.; Bhaduri, S. B. *J. Am. Ceram. Soc.* **2004**, *87*, 2195−2200.
(9) Jiang, H. D.; Liu, X. Y.; Zhang, G.; Li, Y. *J. Biol. Chem.* **2005**, *280*, 42061−42066.
(10) Tjandra, W.; Yao, J.; Ravi, P.; Tam, K. C.; Alamsjah, A. *Chem. Mater.* **2005**, *17*, 4865−4872.
(11) Zhang, H. G.; Zhu, Q. S.; Wang, Y. *Chem. Mater.* **2005**, *17*, 5824−5830.
(12) Nancollas, G. H. *J. Cryst. Growth* **1977**, *42*, 185−193.
(13) LeGeros, R. Z.; Bonel, G.; Legros, R. *Calcif. Tissue Res.* **1978**, *26*, 111−118.
(14) Chow, L. C. *J. Ceram. Soc. Jpn.* **1991**, *99*, 954−964.
(15) Jinawath, S.; Pongkao, D.; Suchanek, W.; Yoshimura, M. *Intl. J. Inorg. Mater.* **2001**, *3*, 997−1001.
(16) Yoshimura, M.; Suda, H.; Okamoto, K.; Ioku, K. *J. Mater. Sci.* **1994**, *29*, 3399−3402.
(17) Hsu, Y. S.; Chang, E.; Liu, H. S. *Ceram. Intl.* **1998**, *24*, 249−254.
(18) Kong, X. D.; Sun, X. D.; Lu, J. B.; Cui, F. Z. *Curr. Appl. Phys.* **2005**, *5*, 519−521.
(19) Da Silva, M. H. P.; Lima, J. H. C.; Soares, G. A.; Elias, C. N.; de Andrade, M. C.; Best, S. M.; Gibson, I. R. *Surf. Coat. Technol.* **2001**, *137*, 270−276.
(20) LeGeros, R. Z.; LeGeros, J. P.; Shirra, W. P. *Adv. X-ray Anal.* **1971**, *14*, 57−66.
(21) Komarneni, S.; Li, D. S.; Newalkar, B.; Katsuki, H.; Bhalla, A. S. *Langmuir* **2002**, *18*, 5959−5962.
(22) Palchik, O.; Kerner, R.; Gedanken, A.; Weiss, A. M.; Slifkin, M. A.; Palchik, V. *J. Mater. Chem.* **2001**, *11*, 874−878.
(23) Grisaru, H.; Palchik, O.; Gedanken, A.; Palchik, V.; Slifkin, M. A.; Weiss, A. M.; Hacohen, Y. R. *Inorg. Chem.* **2001**, *40*, 4814−4815.
(24) Yamamoto, T.; Wada, Y.; Yin, H. B.; Sakata, T.; Mori, H.; Yanagida, S. *Chem. Lett.* **2002**, *31*, 964−965.
(25) Zhu, Y. J.; Wang, W. W.; Qi, R. J.; Hu, X. L. *Angew. Chem., Int. Ed.* **2004**, *43*, 1410−1414.
(26) Vaidhyanathan, B.; Rao, K. J. *Bull. Mater. Sci.* **1996**, *19*, 1163−1165.
(27) Torrent-Burgues, J.; Gomez-Morales, J.; Lopez-Macipe, A.; Rodriguez-Clemente, R. *Cryst. Res. Technol.* **1999**, *34*, 757−762.
(28) Jalota, S.; Tas, A. C.; Bhaduri, S. B. *J. Mater. Res.* **2004**, *19*, 1876−1881.
(29) Penn, R. L.; Oskam, G.; Strathmann, T. J.; Searson, P. C.; Stone, A. T.; Veblen, D. R. *J. Phys. Chem. B* **2001**, *105*, 2177−2182.
(30) Alivisatos, A. P. *Science* **2000**, *289*, 736−737.
(31) Banfield, J. F.; Welch, S. A.; Zhang, H. Z.; Ebert, T. T.; Penn, R. L. *Science* **2000**, *289*, 751−754.
(32) Penn, R. L.; Banfield, J. F. *Geochim. Cosmochim. Acta* **1999**, *63*, 1549−1557.
(33) Panda, R. N.; Hsieh, M. F.; Chung, R. J.; Chin, T. S. *J. Phys. Chem. Solids* **2003**, *64*, 193−199.
(34) Jokanović, V.; Izvonar, D.; Dramićanin, M.; Jokanović, B.; Živojinović, V.; Marković, D.; Dačić, B. *J Mater. Sci. Mater. Med.* **2006**, *17*, 539−546.
(35) Kuriakosea, T. A.; Kalkuraa, S. N.; Palanichamyc, M.; Arivuolid, D.; Dierkse, K.; Bocellif, G.; Betzelb, C. *J. Cryst. Growth* **2004**, *263*, 517−523.